

# How much nuclear physics do we need, to understand the neutrino nucleus cross section ? \*

OMAR BENHAR

INFN and Dipartimento di Fisica, “Sapienza” Università di Roma.  
I-00185 Roma, Italy.

Over the past two decades, electron scattering experiments have clearly exposed the limits of the independent particle model description of atomic nuclei. I will briefly outline the dynamics leading to the appearance of strong correlation effects, and their impact on the electroweak nuclear cross sections in the impulse approximation regime.

PACS numbers: 24.10.Cn,25.30.Fj,61.12.Bt

## 1. Introduction

The theoretical description of nuclear structure and dynamics involves severe difficulties, arising from both the nature of strong interactions and the complexity of the quantum mechanical many-body problem.

In the absence of *ab initio* approaches, one has to resort to nuclear models, based on effective degrees of freedom, protons and neutrons, and phenomenological effective interactions. The available empirical information shows that the nucleon-nucleon (NN) potential exhibits a rich operatorial structure, including spin-isospin dependent and non central components.

Due to the complicated nuclear hamiltonian, the exact solution of the many body Schrödinger equation turns out to be a highly challenging computational task. On the other hand, nuclear systematics suggests that important features of nuclear dynamics can be described using the independent particle model, based on the replacement of the NN potential with a *mean field*. This is in fact the main tenet of the nuclear shell model, which proved exceedingly successful in describing a variety of nuclear properties.

The simplest implementation of the independent particle picture is the Fermi gas (FG) model, in which the nucleus is seen as a degenerate Fermi gas of neutrons and protons, bound with constant energy.

---

\* Presented at the 45th Winter School in Theoretical Physics “Neutrino Interactions: from Theory to Monte Carlo Simulations”, Łańdek-Zdrój, Poland, February 2–11, 2009.

In spite of all the accomplishments of the shell model, it has to be kept in mind that in their classic nuclear physics book, first published in 1952, Blatt and Weisskopf warn the reader that “the limitation of any independent particle model lies in its inability to encompass the correlation between the positions and spins of the various particles in the system” [1].

In recent years, electron scattering experiments have provided overwhelming evidence of correlations in nuclei, whose description requires the use of realistic NN potentials within the formalism of nuclear many-body theory.

In this lectures, after briefly recalling few basic facts on nuclear dynamics beyond the independent particle model, I will discuss the impact of correlation effects on the electroweak nuclear cross sections in the impulse approximation regime.

## 2. Basic facts on nuclear structure and dynamics

One of the most distinctive features of the NN interaction can be inferred from the analysis of the nuclear charge distributions, measured by elastic electron-nucleus scattering experiments.

As shown in Fig. 1, the densities of different nuclei, normalized to the number of protons, exhibit *saturation*, their value in the nuclear interior ( $\rho_0 \sim 0.16 \text{ fm}^{-3}$ ) being nearly constant and independent of the mass number  $A$ . This observation tells us that nucleons cannot be packed together too tightly, thus pointing to the existence of NN *correlations* in coordinate space.

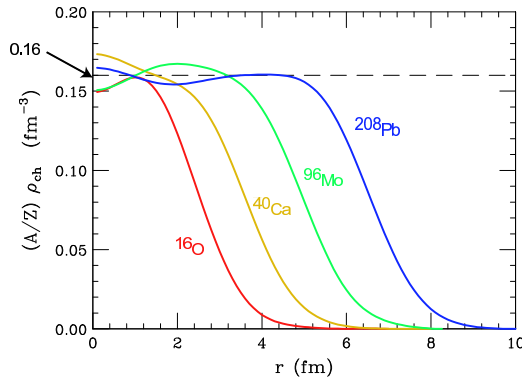


Fig. 1. Radial dependence of the charge density distributions of different nuclei.

Correlations affect the *joint* probability of finding two nucleons at positions  $\mathbf{x}$  and  $\mathbf{y}$ , usually written in the form

$$\rho(\mathbf{x}, \mathbf{y}) = \rho(\mathbf{x})\rho(\mathbf{y})g(\mathbf{x}, \mathbf{y}) , \quad (2.1)$$

where  $\rho(\mathbf{x})$  is the probability of finding a nucleon at position  $\mathbf{x}$ . In the absence of correlations  $g(\mathbf{x}, \mathbf{y}) = 1$ . On the other hand, saturation of nuclear densities indicates that

$$|\mathbf{x} - \mathbf{y}| \lesssim r_c \implies g(\mathbf{x}, \mathbf{y}) \ll 1, \quad (2.2)$$

$r_c$  being the correlation range.

Nucleons obey Fermi statistics, and may therefore repel one another even in the absence of dynamical interactions. To see this, consider a degenerate FG consisting of equal number of protons and neutrons at uniform density  $\rho$ . In this case Eq.(2.1) reduces to

$$\rho(|\mathbf{x} - \mathbf{y}|) = \rho^2 g_F(|\mathbf{x} - \mathbf{y}|), \quad (2.3)$$

with the correlation function  $g_F(x)$  displayed by the dashed line in Fig. 2. It clearly appears that the effects of statistical correlations, while being clearly visible, is not too strong. The probability of finding two nucleons at relative distance  $x \ll 1$  fm is still very large.

In the early days of nuclear physics, just after the neutron had been discovered and the existence of neutron stars had been proposed, Tolman, Oppenheimer and Volkoff [2, 3] carried out the first studies of the stability of neutron stars, modeled as a gas of noninteracting particles at zero temperature. Their work was aimed at determining whether the degeneracy pressure, resulting from the repulsion induced by Pauli exclusion principle, could become strong enough to balance the gravitational pull, thus giving rise to a stable star. These calculations led to predict a maximum neutron star mass  $\sim 0.8 M_\odot$ ,  $M_\odot$  being the mass of the sun, to be compared to the results of most experimental measurements yielding values  $\sim 1.4 M_\odot$ . The observation of neutron stars with masses largely exceeding the upper limit determined in Refs.[2, 3] can be regarded as a striking evidence of the failure of the description of nuclear systems based on the FG model. To explain the observed neutron stars masses, the effects of nuclear dynamics have to be explicitly taken into account.

The strength of *dynamical* NN correlations is illustrated by the solid line of Fig. 2, showing the NN radial correlation function in nuclear matter at uniform density  $\rho_0 = 0.16 \text{ fm}^{-3}$ , obtained from the variational approach discussed in the Section 4. Comparison with the dashed line, computed including statistical correlations only, clearly shows that the dynamical effects dominate.

### 3. The nucleon-nucleon interaction

The NN interaction can be best studied in the two-nucleon system. There is only one NN bound state, the nucleus of deuterium, or deuteron, consisting

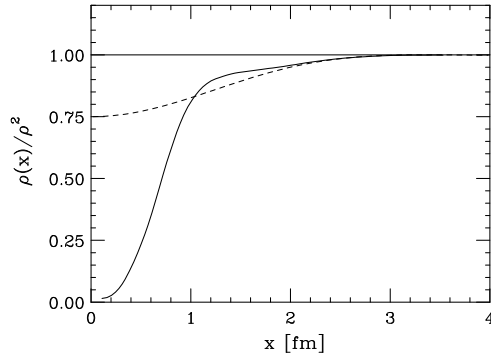


Fig. 2. Spin-isospin averaged NN radial correlation function in isospin symmetric nuclear matter at uniform density  $\rho_0 = 0.16 \text{ fm}^{-3}$ . The solid line shows the full result of the calculation of Ref. [4], while the dashed line only includes statistical correlations.

of a proton and a neutron coupled to total spin and isospin  $S = 1$  and  $T = 0$ , respectively. This is clear manifestation of the fact that nuclear forces are *spin-isospin dependent*.

Another important piece of information can be inferred from the observation that the deuteron exhibits a nonvanishing electric quadrupole moment, implying that its charge distribution is not spherically symmetric. Hence, the NN interaction is *noncentral*.

Besides the properties of the two-nucleon bound state, the large data set of phase shifts measured in NN scattering experiments ( $\sim 4000$  data points, corresponding to energies up to pion production threshold) provides valuable additional information on the nature of NN forces.

Back in the 1930s, Yukawa suggested that nuclear interactions were mediated by a particle of mass  $\sim 100 \text{ MeV}$ , that was later identified with the pion. The one pion exchange (OPE) mechanism provides a fairly accurate description of the long range behavior of the NN interaction, as it explains the measured NN scattering phase shifts in states of high angular momentum.

At intermediate and short range more complicated processes, involving the exchange of two or more pions (possibly interacting among themselves) or heavier particles, like the  $\rho$  and  $\omega$  mesons, have to be taken into account. Moreover, when their relative distance becomes very small ( $\lesssim 0.5 \text{ fm}$ ) nucleons, being composite and finite in size, are expected to overlap. In this regime, NN interactions should in principle be described in terms of interactions between nucleon constituents, i.e. quarks and gluons, as dictated by quantum chromodynamics (QCD), which is believed to be the fundamental theory of strong interactions.

Phenomenological potentials describing the *full* NN interaction are generally written in the form

$$v = v_\pi + v_R , \quad (3.1)$$

where  $v_\pi$  is the OPE potential, while  $v_R$  describes the interaction at intermediate and short range.

The spin-isospin dependence and the noncentral nature of the potential can be properly accounted for rewriting Eq. (3.1) in the form

$$v_{ij} = \sum_{ST} [v_{TS}(r_{ij}) + \delta_{S1}v_{tT}(r_{ij})S_{ij}] P_S \Pi_T , \quad (3.2)$$

where  $S$  and  $T$  denote the total spin and isospin of the interacting pair,  $P_S$  and  $\Pi_T$  are the corresponding projection operators and

$$S_{ij} = \frac{3}{r_{ij}^2} (\boldsymbol{\sigma}_i \cdot \mathbf{r}_{ij})(\boldsymbol{\sigma}_j \cdot \mathbf{r}_{ij}) - (\boldsymbol{\sigma}_i \cdot \boldsymbol{\sigma}_j) , \quad (3.3)$$

reminiscent of the operator describing the interaction between two magnetic dipoles, accounts for the presence of non central contributions.

The functions  $v_{TS}(r_{ij})$  and  $v_{tT}(r_{ij})$  describe the radial dependence of the interaction in the different spin-isospin channels, and reduce to the corresponding components of the OPE potential at large  $r_{ij}$ . Their shapes are chosen in such a way as to reproduce the available NN data (deuteron binding energy, charge radius and quadrupole moment and the NN scattering phase shifts).

As an example, Fig. 3 shows the potential acting between two nucleons with  $S = 0$  and  $T = 1$ . The presence of the repulsive core inducing strong short range correlations (compare to Fig. 2) is apparent.

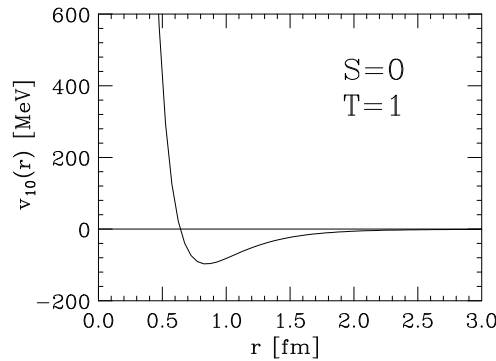


Fig. 3. Radial dependence of the NN potential describing the interaction between two nucleons in the state of total spin and isospin  $S = 0$  and  $T = 1$ .

Although state-of-the-art parametrizations of the NN potential [5] have a more complex operatorial structure, including non static and charge symmetry breaking components, the simple form (3.2) has the advantage of being easily applicable, and still allows one to obtain a reasonable description of the two-nucleon bound and scattering states.

#### 4. Nuclear many body theory

According to the *paradigm* of nuclear many-body theory (NMBT) the nucleus can be viewed as a collection of  $A$  pointlike protons and neutrons, whose dynamics are described by the nonrelativistic hamiltonian

$$H = \sum_i \frac{\mathbf{p}_i^2}{2m} + \sum_{j>i} v_{ij} + \sum_{k>j>i} V_{ijk} , \quad (4.1)$$

where  $\mathbf{p}_i$  and  $m$  denote the momentum of the  $i$ -th nucleon and its mass, respectively. The determination of the two-body potential  $v_{ij}$  has been outlined in the previous section. The inclusion of the three-nucleon interaction, whose contribution to the energy satisfies  $\langle V_{ijk} \rangle \ll \langle v_{ij} \rangle$ , is required to account for the binding energy of the three-nucleon systems [6].

It is very important to realize that in NMBT the dynamics is fully specified by the properties of *exactly solvable* system, having  $A \leq 3$ , and does not suffer from the uncertainties involved in many body calculations. Once the nuclear hamiltonian is fixed, calculations of nuclear observables for a variety of systems, ranging from the deuteron to neutron stars, can be carried out without making use of any adjustable parameters.

The predictive power of the dynamical model based on the hamiltonian of Eq.(4.1) has been extensively tested by computing the energies of the ground and low-lying excited states of nuclei with  $A \leq 12$ . The results of these studies, in which the many body Schrödinger equation is solved *exactly* using stochastic methods, turn out to be in excellent agreement with experimental data [7].

Accurate calculations can also be carried out for uniform nuclear matter, exploiting translational invariance and using the stochastic method [8], the variational approach [9], or G-matrix perturbation theory [10].

In the variational approach, the nuclear states are written in such a way as to incorporate the correlation structure induced by NN interactions. In the case of uniform nuclear matter, they can be obtained from the states of the noninteracting FG through the transformation

$$|n\rangle = F|n_{FG}\rangle , \quad (4.2)$$

with  $F$  written in the form

$$F = \mathcal{S} \prod_{ij} f_{ij} . \quad (4.3)$$

The structure of the two-body correlation operator  $f_{ij}$  reflects the complexity of the NN potential, described by Eq.(3.2), while the symmetrization operator  $\mathcal{S}$  is needed to account for the fact that  $[f_{ij}, f_{jk}] \neq 0$ . The shapes of the radial functions  $f_{TS}(r_{ij})$  and  $f_{tT}(r_{ij})$  are determined by functional minimization of the expectation value of the hamiltonian (4.1) in the correlated ground state.

The formalism based on correlated wave functions is ideally suited to carry out calculations of nuclear matter properties strongly affected by correlation effects.

The hole spectral function  $P_h(\mathbf{k}, E)$ , yielding the probability of removing a nucleon of momentum  $\mathbf{k}$  from the nuclear ground state leaving the residual system with excitation energy  $E$  [11], can be written in the form

$$P_h(\mathbf{k}, E) = \frac{1}{\pi} \frac{Z_k^2 \text{Im}\Sigma(\mathbf{k}, \epsilon_k)}{(E + \epsilon_k)^2 + [Z_k \text{Im} \Sigma(\mathbf{k}, \epsilon_k)]^2} + P_h^B(\mathbf{k}, E) , \quad (4.4)$$

with  $\epsilon_k$  defined by the equation

$$\epsilon_k = \epsilon_k^0 + \text{Re} \Sigma(\mathbf{k}, \epsilon_k) , \quad (4.5)$$

where  $\epsilon_k^0 = |\mathbf{k}|^2/2m$  and  $\Sigma(\mathbf{k}, E)$  is the nucleon self energy.

The first term in the right hand side of equation (4.4) describes the spectrum of a system of independent *quasiparticles* of momentum  $|\mathbf{k}| < k_F$ ,  $k_F$  being the Fermi momentum, moving in a complex mean field whose real and imaginary parts determine the quasiparticle effective mass and lifetime, respectively. In the FG model this term shrinks to a  $\delta$ -function and  $Z_k = 1$ . The presence of the second term is a pure correlation effect. In the FG model  $P_h^B(\mathbf{k}, E) = 0$ , while in the presence of interactions the correlation term is the only one providing a nonvanishing contribution at  $|\mathbf{k}| > k_F$ .

Figure 4 illustrates the energy dependence of the hole spectral function of nuclear matter, calculated in Ref.[11] using the correlated basis approach. Comparison with the FG model clearly shows that the effects of nuclear dynamics and NN correlations are large, resulting in a shift of the quasiparticle peaks, whose finite width becomes large for deeply-bound states with  $|\mathbf{k}| \ll k_F$ . In addition, NN correlations are responsible for the appearance of strength at  $|\mathbf{k}| > k_F$ .

The results of nuclear matter calculations have been extensively employed to obtain the hole spectral functions of heavy nuclei within the local density approximation (LDA) [12].

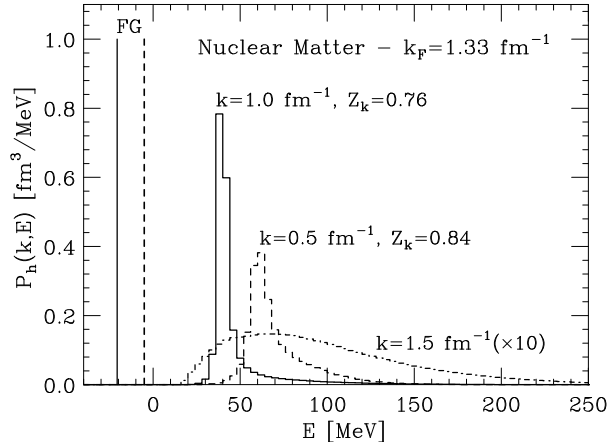


Fig. 4. Energy dependence of the hole spectral function of nuclear matter at equilibrium density, corresponding to  $k_F = 1.33 \text{ fm}^{-1}$ . The solid, dashed and dot-dash lines correspond to  $|\mathbf{k}| = 1, 0.5$  and  $1.5 \text{ fm}^{-1}$ , respectively. The FG spectral function at  $|\mathbf{k}| = 1$  and  $0.5 \text{ fm}^{-1}$  is shown for comparison.

### 5. Nuclear response to a scalar probe

Within NMBT, the nuclear response to a scalar probe delivering momentum  $\mathbf{q}$  and energy  $\omega$  can be written in terms of the imaginary part of the particle-hole propagator  $\Pi(\mathbf{q}, \omega)$  according to [13, 14]

$$S(\mathbf{q}, \omega) = \frac{1}{\pi} \text{Im} \Pi(\mathbf{q}, \omega) = \frac{1}{\pi} \text{Im} \langle 0 | \rho_{\mathbf{q}}^\dagger \frac{1}{H - E_0 - \omega - i\eta} \rho_{\mathbf{q}} | 0 \rangle, \quad (5.1)$$

where  $\eta = 0^+$ ,  $\rho_{\mathbf{q}} = \sum_{\mathbf{k}} a_{\mathbf{k}+\mathbf{q}}^\dagger a_{\mathbf{k}}$  is the operator describing the fluctuation of the target density induced by the interaction with the probe,  $a_{\mathbf{k}}^\dagger$  and  $a_{\mathbf{k}}$  are nucleon creation and annihilation operators, and  $|0\rangle$  is the target ground state, satisfying the Schrödinger equation  $H|0\rangle = E_0|0\rangle$ .

In general, the calculation of the response requires the knowledge of the spectral functions associated with both particle and hole states, as well as of the particle-hole effective interaction [14, 15]. The spectral functions are mostly affected by short range NN correlations (see Fig. 4), while the inclusion of the effective interaction, e.g. within the framework of the Tamm Dancoff and Random Phase Approximation [15, 16], is needed to account for collective excitations induced by long range correlations, involving more than two nucleons.

At large momentum transfer, as the space resolution of the probe becomes small compared to the average NN separation distance,  $S(\mathbf{q}, \omega)$  is no

longer significantly affected by long range correlations [16]. In this kinematical regime the zero-th order approximation in the effective interaction, is expected to be applicable. The response reduces to the incoherent sum of contributions coming from scattering processes involving a single nucleon, and can be written in the simple form

$$S(\mathbf{q}, \omega) = \int d^3k dE P_h(\mathbf{k}, E) P_p(\mathbf{k} + \mathbf{q}, \omega - E) . \quad (5.2)$$

The widely employed impulse approximation (IA) can be readily obtained from the above definition replacing  $P_p$  with the prediction of the FG model, which amounts to disregarding final state interactions (FSI) between the struck nucleon and the spectator particles. The resulting expression reads

$$S_{IA}(\mathbf{q}, \omega) = \int d^3k dE P_h(\mathbf{k}, E) \theta(|\mathbf{k} + \mathbf{q}| - k_F) \delta(\omega - E - \epsilon_{|\mathbf{k} + \mathbf{q}|}^0) . \quad (5.3)$$

Figure 5, showing the  $\omega$  dependence of the nuclear matter response function at  $|\mathbf{q}| = 5 \text{ fm}^{-1}$ , illustrates the role of correlations in the target initial state. The solid and dashed lines have been obtained from Eq.(5.3), using the spectral function of Ref.[11], and the from the FG model, respectively. It is apparent that the inclusion of correlations produces a significant shift of the strength towards larger values of energy transfer.

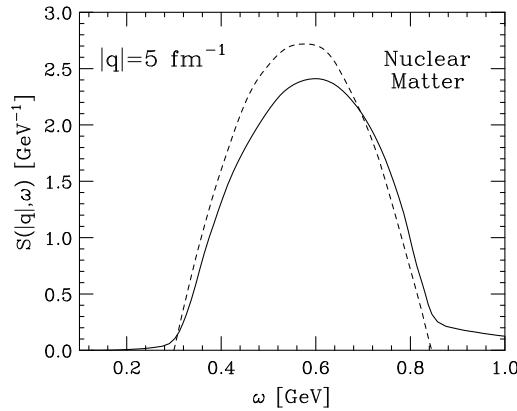


Fig. 5. Nuclear matter  $S_{IA}(\mathbf{q}, \omega)$  (see Eq.(5.3)), as a function of  $\omega$  at  $|\mathbf{q}| = 5 \text{ fm}^{-1}$ . The solid and dashed lines correspond to the spectral function of Ref.[11] and to the FG model, respectively.

Obvioulsy, at large  $\mathbf{q}$  the calculation of  $P_p(\mathbf{k} + \mathbf{q}, \omega - E)$  cannot be carried out using a nuclear potential model. However, it can be obtained form the measured NN scattering amplitude within the eikonal approximation. A

systematic scheme to include corrections to Eq.(5.3) and take into account FSI has been developed in Ref.[17]. The main effects of FSI on the response are i) a shift in energy, due to the mean field of the spectator nucleons and ii) a redistributions of the strength, due to the coupling of the one particle-one hole final state to  $n$  particle- $n$  hole final states.

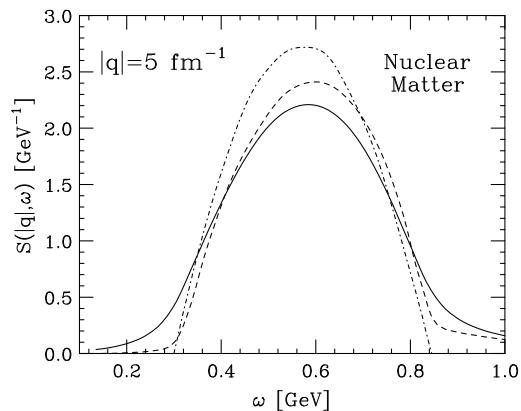


Fig. 6. Nuclear matter  $S(\mathbf{q}, \omega)$  as a function of  $\omega$  at  $|\mathbf{q}| = 5 \text{ fm}^{-1}$ . The solid and dashed lines have been obtained from the spectral function of Ref. [11], with and without inclusion of FSI, respectively. The dot-dash line corresponds to the FG model.

Figure 6 shows the  $\omega$  dependence of the nuclear matter response of Eqs.(5.2) and (5.3) at  $|\mathbf{q}| = 5 \text{ fm}^{-1}$ . The solid and dashed lines have been obtained using the spectral function of Ref.[11], with and without inclusion of FSI according to the formalism of Ref.[17], respectively. For reference, the results of the FG model are also shown by the dot-dash line. The two effects of FSI, energy shift and redistribution of the strength from the region of the peak to the tails, clearly show up in the comparison between solid and dashed lines.

## 6. Electron-nucleus cross section

The differential cross section of the process

$$e + A \rightarrow e' + X , \quad (6.1)$$

in which an electron of initial four-momentum  $k_e \equiv (E_e, \mathbf{k}_e)$  scatters off a nuclear target to a state of four-momentum  $k'_e \equiv (E_{e'}, \mathbf{k}_{e'})$ , the target final state being undetected, can be written in Born approximation as

$$\frac{d^2\sigma}{d\Omega_{e'} dE_{e'}} = \frac{\alpha^2}{Q^4} \frac{E_{e'}}{E_e} L_{\mu\nu} W^{\mu\nu} , \quad (6.2)$$

where  $\alpha = 1/137$  is the fine structure constant,  $d\Omega_{e'}$  is the differential solid angle in the direction specified by  $\mathbf{k}_{e'}$ ,  $Q^2 = -q^2$  and  $q = k_e - k_{e'} \equiv (\omega, \mathbf{q})$  is the four momentum transfer.

The tensor  $L_{\mu\nu}$  is fully specified by the measured electron kinematical variables. All the information on target structure is contained in the tensor  $W^{\mu\nu}$ , whose definition involves the initial and final nuclear states  $|0\rangle$  and  $|X\rangle$ , carrying four-momenta  $p_0$  and  $p_X$ , as well as the nuclear current operator  $J^\mu$ :

$$W^{\mu\nu} = \sum_X \langle 0 | J^\mu | X \rangle \langle X | J^\nu | 0 \rangle \delta^{(4)}(p_0 + q - p_X) , \quad (6.3)$$

where the sum includes all hadronic final states. Note that the tensor of Eq.(6.3) is the generalization of the nuclear response, discussed in the previous section, to the case of a probe interacting with the target through a vector current. To see this, insert the complete set of eigenstates of the nuclear hamiltonian in the definition of Eq.(5.1). The result is

$$S(\mathbf{q}, \omega) = \sum_n \langle 0 | \rho_{\mathbf{q}}^\dagger | n \rangle \langle n | \rho_{\mathbf{q}} | 0 \rangle \delta(\omega + E_0 - E_n) , \quad (6.4)$$

to be compared to Eq.(6.3).

In the IA regime, the nuclear current appearing in Eq. (6.3) can be written as a sum of one-body currents

$$J^\mu \rightarrow \sum_i j_i^\mu , \quad (6.5)$$

while  $|X\rangle$  reduces to the direct product of the hadronic state produced at the electromagnetic vertex, carrying four momentum  $p_x \equiv (E_x, \mathbf{p}_x)$ , and the state describing the residual system, carrying momentum  $\mathbf{p}_{\mathcal{R}} = \mathbf{q} - \mathbf{p}_x$ .

As a result, the Eq. (6.3) can be rewritten in the form ( $k \equiv (E, \mathbf{k})$ )

$$W^{\mu\nu}(\mathbf{q}, \omega) = \int d^4k \left( \frac{m}{E_{\mathbf{k}}} \right) \left[ Z P_p(k) w_p^{\mu\nu}(\tilde{q}) + N P_n(k) w_n^{\mu\nu}(\tilde{q}) \right] , \quad (6.6)$$

where  $Z$  and  $N = A - Z$  are the number of target protons and neutrons, while  $P_p$  and  $P_n$  denote the proton and neutron *hole* spectral functions, respectively. In Eq. (6.6),  $E_{\mathbf{k}} = \sqrt{|\mathbf{k}^2| + m^2}$  and

$$w_N^{\mu\nu} = \sum_x \langle \mathbf{k}, N | j_N^\mu | x, \mathbf{k} + \mathbf{q} \rangle \langle \mathbf{k} + \mathbf{q}, x | j_N^\nu | N, \mathbf{k} \rangle \delta(\tilde{\omega} + E_{\mathbf{k}} - E_x) . \quad (6.7)$$

The tensor  $w_n^{\mu\nu}$  describes the electromagnetic structure of a nucleon of initial momentum  $\mathbf{k}$  in *free space*. The effect of nuclear binding is accounted for by the replacement  $\omega \rightarrow \tilde{\omega}$ , with [18]

$$\tilde{\omega} = E_x - E_{\mathbf{k}} = \omega - E + m - E_{\mathbf{k}} . \quad (6.8)$$

The above equations show that within the IA scheme, the definition of the electron-nucleus cross section involves two elements: i) the tensor  $w_N^{\mu\nu}$ , that can be extracted from electron-proton and electron-deuteron data, and ii) the spectral function, discussed in the Section 4.

The formalism of NMBT has been extensively employed in the analysis of a variety of electron-nucleus scattering observables. In Ref. [19], it has been employed to calculate the inclusive electron scattering cross sections off oxygen, at beam energies ranging between 700 and 1200 MeV and electron scattering angle  $32^\circ$ . In this kinematical region single nucleon knock out is the dominant reaction mechanism and both quasi-elastic and inelastic processes, leading to the appearance of nucleon resonances, must be taken into account.

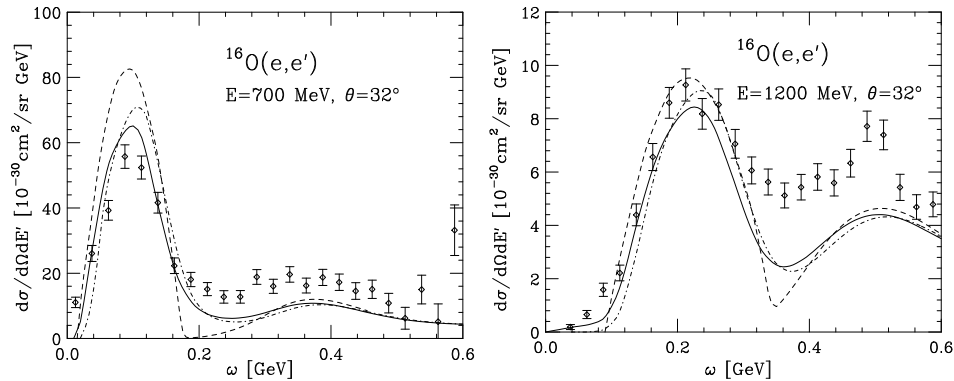


Fig. 7. Cross section of the process  $^{16}\text{O}(e, e')$  at scattering angle  $32^\circ$  and beam energy 700 MeV (left panel) and 1200 MeV (right panel), as a function of the electron energy loss  $\omega$ . Solid lines: full calculation, including FSI. Dot-dash lines: IA calculation. Dashed lines: FG model. The data are taken from Ref.[20]

The comparison between theory and the experiment, in Fig. 7, shows that the data in the region of the quasi-elastic peak are accounted for with an accuracy better than  $\sim 10\%$ . The discrepancies observed at larger electron energy loss, where  $\Delta$  production dominates, can be ascribed to deficiencies in the description of the nucleon structure functions [21]. For reference, the predictions of the FG model are also displayed by dashed lines. A realistic description of nuclear dynamics clearly appears to be needed to explain the measured cross sections.

## 7. Charged current neutrino-nucleus cross section

The cross section of the weak charged current process  $\nu_\ell + A \rightarrow \ell^- + X$  can be written in the form (compare to Eq. (6.2))

$$\frac{d^2\sigma}{d\Omega_\ell dE_\ell} = \frac{G_F^2 V_{ud}^2}{16\pi^2} \frac{|\mathbf{k}_\ell|}{|\mathbf{k}|} L_{\mu\nu} W_A^{\mu\nu}, \quad (7.1)$$

where  $G_F$  is the Fermi constant,  $V_{ud}$  is the CKM matrix element coupling  $u$  and  $d$  quarks and  $\mathbf{k}$  and  $\mathbf{k}_\ell$  denote the momenta of the incoming neutrino and the outgoing charged lepton, respectively.

The formalism outlined in the previous section can be readily generalized to the case of neutrino-nucleus interactions, the required nuclear physics input being the same in the two instances. On the other hand, while the vector form factors entering the definition of the electron-nucleus cross section can be measured with great accuracy using proton and deuteron targets, the experimental determination of the nucleon axial form factor is still somewhat controversial, as different experiments report appreciably different results [22, 23, 24, 25]. In these lectures, I will focus on the role of nuclear dynamics, and do not discuss the uncertainty associated with the weak form factor.

In order to gauge the magnitude of nuclear effects, in Fig. 8 the energy dependence of the quasi elastic contribution to the total cross section of the process  $\nu_e + {}^{16}\text{O} \rightarrow e^- + X$  computed using different approximations are compared [26]. The dot-dash line represents the result obtained describing oxygen as a collection of noninteracting stationary nucleons, while the dashed and solid lines have been obtained from the FG model and using the spectral function of Ref. [12], respectively. It is apparent that replacing the FG with the approach based on a realistic spectral function leads to a sizable suppression of the total cross section. Comparison between the dot-dash line and the dotted one, obtained taking into account the effect of Pauli blocking [19], shows that the overall change due to nuclear effect is  $\sim 20\%$ .

Note that FSI between the nucleon produced at the elementary weak interaction vertex and the spectator particles have not been taken into account, as they *do not* contribute to the total cross section.

To see how much the description of nuclear dynamics may affect the data analysis of neutrino oscillation experiments, consider reconstruction of the incoming neutrino energy in charged current quasi elastic events  $\nu_\mu + A \rightarrow \mu + p + (A-1)$ , in which the muon energy,  $E_\mu$ , and angle,  $\theta_\mu$ , are measured.

From the requirement that the elementary scattering process be elastic, it follows that the neutrino energy is given by

$$E_\nu = \frac{m_p^2 - m_\mu^2 - E_n^2 + 2E_\mu E_n - 2\mathbf{k}_\mu \cdot \mathbf{p}_n + |\mathbf{p}_n^2|}{2(E_n - E_\mu + |\mathbf{k}_\mu| \cos \theta_\mu - |\mathbf{p}_n| \cos \theta_n)}, \quad (7.2)$$

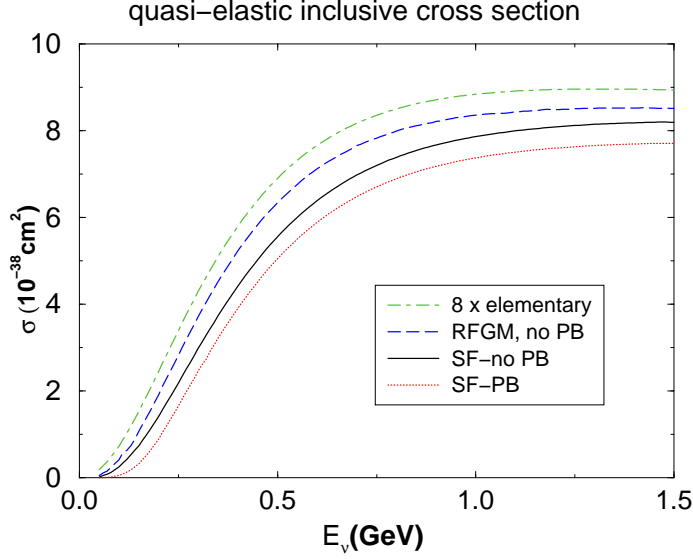


Fig. 8. Total quasi-elastic cross section of the process  $\nu_e + {}^{16}\text{O} \rightarrow e^- + X$ . The dot-dash line represents eight times the elementary cross section; the dashed line is the result of the FG model; the dotted and solid lines have been obtained using the spectral function of Ref. [12], with and without inclusion of Pauli blocking, respectively.

where  $m_p$  and  $m_\mu$  denote the proton and muon mass, respectively,  $\mathbf{k}_\mu$  is the muon momentum and  $\mathbf{p}_n$  and  $E_n$  are the momentum and energy carried by the struck neutron.

Setting  $|\mathbf{p}_n| = 0$  and fixing the neutron removal energy to a constant value  $\epsilon$ , i.e. setting  $E_n = m_n - \epsilon$ ,  $m_n$  being the neutron mass, Eq.(7.2) reduces to

$$E_\nu = \frac{2E_\mu(m_n - \epsilon) - (\epsilon^2 - 2m_n\epsilon + m_\mu^2 + \Delta m^2)}{2(m_n - \epsilon - E_\mu + |\mathbf{k}_\mu| \cos \theta_\mu)}, \quad (7.3)$$

with  $\Delta m^2 = m_n^2 - m_p^2$ . In the analysis of Refs. [23, 24] the energy of the incoming neutrino has been reconstructed using the above equation.

The differences between the  $E_\nu$  predicted by the approach based on a realistic spectral function and that obtained from the FG model is illustrated in Fig. (9), where the values obtained from Eq. (7.3) are also shown by arrows. The appearance of the tail extending to large  $E_\nu$ , to be ascribed to NN correlations not included in the FG model, leads to a sizable increase of the average neutrino energy.

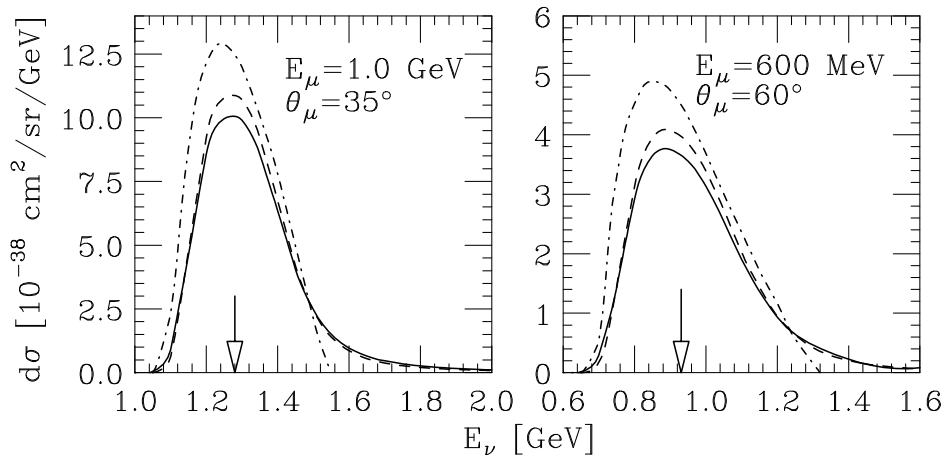


Fig. 9. Right panel: Differential cross section of the process  $\nu_\mu + A \rightarrow \mu + p + (A-1)$ , at  $E_\mu = 600$  MeV and  $\theta_\mu = 60^\circ$ , as a function of the incoming neutrino energy. The solid line shows the results of the full calculation, carried out within the approach of Refs. [19, 26], whereas the dashed line has been obtained neglecting the effects of FSI. The dot-dash line corresponds to the FG model. The arrow points to the value of  $E_\nu$  obtained from Eq. (7.3). Left panel: Same as the right panel, but for  $E_\mu = 1$  GeV and  $\theta_\mu = 35^\circ$ .

## 8. Conclusions

Dynamical correlation effects, which are long known to play a critical role in shaping the nuclear response to electromagnetic probes, are also important in neutrino-nucleus interactions.

Although the answer to the question addressed in the title of these lectures is somewhat context dependent, as not all the observables measured in neutrino experiments are equally sensitive to NN correlations, there are instances in which a realistic description of nuclear structure and dynamics is badly needed. For example, analyses aimed at extracting *nucleon* properties, such as the axial form factor, from *nuclear* cross sections require a fully quantitative control of nuclear effects.

The formalism based on NMBT, which proved very effective in theoretical studies of electron-nucleus scattering, can be easily generalized to the case of weak interactions. The implementation of realistic spectral functions in the Monte Carlo simulation codes, which would significantly improve the description of the initial state, does not involve severe difficulties. As far as final states are concerned, a consistent description of FSI effects is available for the case of quasielastic scattering, which is the dominant reaction mechanism at beam energies around 1 GeV. The extension to the case of pion

production and deep inelastic scattering is certainly possible, and is being actively investigated.

## REFERENCES

- [1] J.M. Blatt and V.F. Weisskopf, *Theoretical Nuclear Physics*, (Dover, New York, 1979) p. 291.
- [2] R. C. Tolman, Phys. Rev. **55** (1939) 364.
- [3] J. R. Oppenheimer e G. M. Volkoff, Phys. Rev. **55** (1939) 374.
- [4] R. Schiavilla *et al*, Nucl. Phys. A **473** 267 (1987) 267.
- [5] R.B. Wiringa , V.G.J. Stoks, R. Schiavilla, Phys. Rev. **C51** (1995) 38.
- [6] P.S. Pudliner *et al*, Phys. Rev. **C56** (1997) 1720.
- [7] S.C. Pieper and R.B. Wiringa, Ann. Rev. Nucl. Part. Sci. **51** (2001) 53.
- [8] K. S. A. Sarsa, S. Fantoni, and F. Pederiva, Phys. Rev. C **68** (2003) 024308.
- [9] A. Akmal, V. Pandharipande, and D. Ravenhall, Phys. Rev. C **58** (1998) 1804.
- [10] M. Baldo *et al*, Phys. Lett. B **473** (2000) 1.
- [11] O. Benhar, A. Fabrocini and S. Fantoni, Nucl. Phys. A **505** (1989) 267.
- [12] O. Benhar *et al*, Nucl. Phys. A **579** (1994) 493.
- [13] A. Fetter, and J. Walecka, *Quantum Theory of Many Particle Systems*, (McGraw-Hill, New York, 1971).
- [14] O. Benhar, A. Fabrocini, and S. Fantoni, Nucl. Phys. A **550** (1992) 201.
- [15] W. Dickhoff, and C. Barbieri, Prog. Part. Nucl. Phys. **52** (2004) 377.
- [16] O. Benhar and N. Farina, Physics Letters B, in press [arXiv:0904.2260].
- [17] O. Benhar *et al*, Phys. Rev. C **44** (1991) 2328.
- [18] O. Benhar, D. Day and I. Sick, Rev. Mod. Phys. **80** (2008) 189.
- [19] O. Benhar *et al*, *Phys. Rev. D* **72** (2005) 053005.
- [20] M. Anghinolfi *et al.*, Nucl. Phys. A **602** (1996) 405.
- [21] O. Benhar and D. Meloni, *Phys. Rev. Lett.* **97** (2006) 192301.
- [22] V. Bernard *et al.*, J. Phys. G **28** (2002) R1.
- [23] R. Gran *et al.* (K2K Collaboration), Phys. Rev. D **74**, (2006) 052002.
- [24] A.A. Aguilar Arevalo *et al.* (MiniBooNE), Phys. Rev. Lett. **100** (2008) 032301.
- [25] NOMAD Collaboration, V. Lyubushkin *et al*, arXiv:0812.4543
- [26] O. Benhar and D. Meloni, Nucl. Phys. A **789** (2007) 379.